The Company of
Biologists

RESEARCH ARTICLE

Bristles reduce the force required to 'fling' wings apart in the smallest insects

Shannon K. Jones[1],*, Young J. J. Yun[1], Tyson L. Hedrick[2], Boyce E. Griffith[1,3] and Laura A. Miller[1,2]

ABSTRACT

The smallest flying insects commonly possess wings with long bristles. Little quantitative information is available on the morphology of these bristles, and their functional importance remains a mystery. In this study, we (1) collected morphological data on the bristles of 23 species of Mymaridae by analyzing high-resolution photographs and (2) used the immersed boundary method to determine via numerical simulation whether bristled wings reduced the force required to fling the wings apart while still maintaining lift. The effects of Reynolds number, angle of attack, bristle spacing and wing–wing interactions were investigated. In the morphological study, we found that as the body length of Mymaridae decreases, the diameter and gap between bristles decreases and the percentage of the wing area covered by bristles increases. In the numerical study, we found that a bristled wing experiences less force than a solid wing. The decrease in force with increasing gap to diameter ratio is greater at higher angles of attack than at lower angles of attack, suggesting that bristled wings may act more like solid wings at lower angles of attack than they do at higher angles of attack. In wing–wing interactions, bristled wings significantly decrease the drag required to fling two wings apart compared with solid wings, especially at lower Reynolds numbers. These results support the idea that bristles may offer an aerodynamic benefit during clap and fling in tiny insects.

KEY WORDS: Insect flight, Biomechanics, Clap and fling, Intermediate Reynolds numbers, Computational fluid dynamics, Immersed boundary method

INTRODUCTION

Unlike larger insects, the smallest flying insects commonly possess wings with long bristles on the fringes. Because insect wing bristles are not well studied, their physiological or mechanical importance remains a mystery. Bristles on insect wings could serve many different functions: reducing the weight of the insect (Sunada et al., 2002), providing an aerodynamic benefit (Davidi and Weihs, 2012; Santhanakrishnan et al., 2014), enhancing electrostatic charges to help in dispersal, similar to what has been suggested for spiders (Gorham, 2013 preprint), helping to fold and unfold the wings (Ellington, 1980), or acting as mechanosensory structures, similar to those in *Drosophila* (Valmalette et al., 2015). The last two roles, however, are not universal as most parasitoid wasps do not have hinges for folding and unfolding the bristles and it is not clear that all bristles are innervated. In this study, we investigated the aerodynamic role that bristles may play in wing–wing interactions.

The fluid dynamics of flow through bristled appendages similar to those on the wings of small insects has been explored with physical (Loudon et al., 1994; Sunada et al., 2002), analytical (Cheer and Koehl, 1987; Koehl,1993) and numerical models (Barta and Weihs, 2006; Weihs and Barta, 2008; Barta, 2011; Davidi and Weihs, 2012). Previous analytical studies, however, have only considered cases with 2–4 bristles, and most numerical studies have assumed Stokes flow and did not consider wing–wing interactions.

Thysanoptera, Trichogrammatidae, Mymaridae, Ptiliidae, Cecidomyiidae, Ceratopogonidae and Nepticulidae all include species that have bristled wings. Little information, however, is available on the diameter, spacing and bristle-based Reynolds number (Re_b) on tiny insect wings. Re_b is defined as follows:

$$Re_b = \frac{\rho U D}{\mu}, \tag{1}$$

in which ρ is the fluid density, U is the average wingtip velocity, D is the bristle diameter and μ is the dynamic viscosity. The bristles on the wings of *Encarsia formosa* (Ellington, 1975) and *Thrips physapus* (Kuethe, 1975) function near $Re_b = 7\times10^{-2}$ and 1×10^{-2}, respectively, whereas the chord-based Reynolds number (Re_c) for these insects is of the order of 10. The gap spacing to bristle diameter ratios (G/D) are 5:1 and 10:1, respectively (Ellington, 1975, 1980).
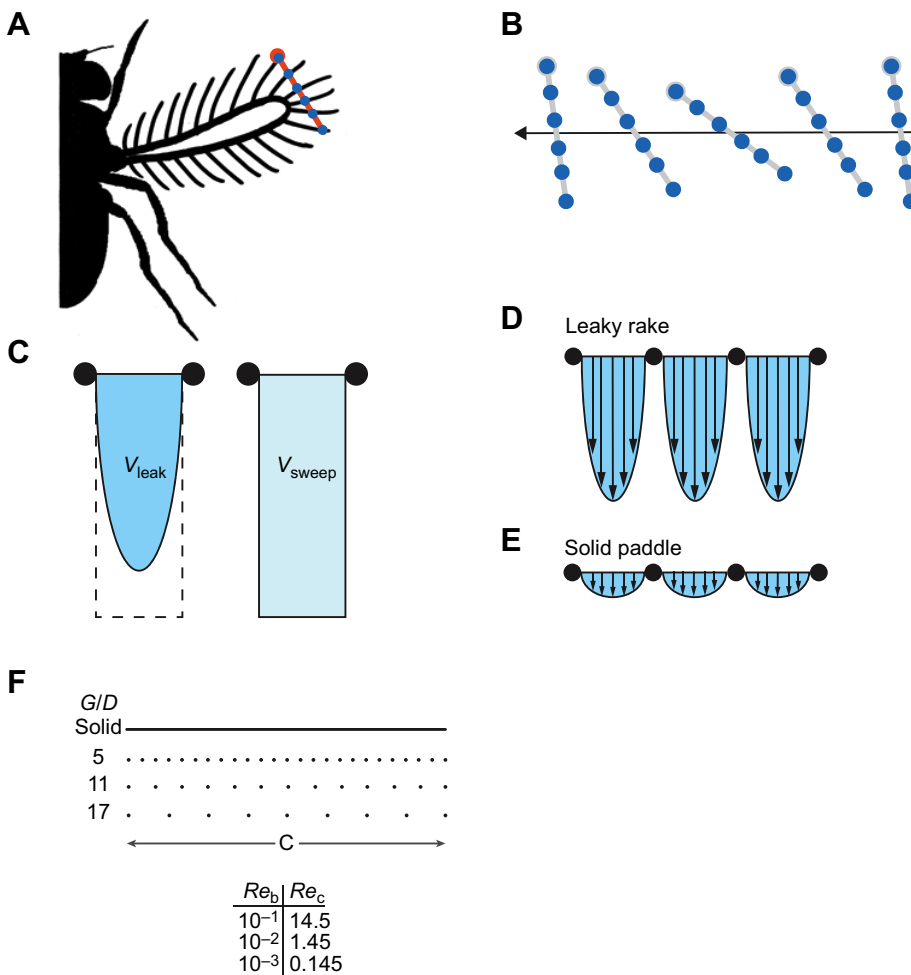
Computational fluid dynamics provides a convenient way to model a row of bristles. The bristles on insect wings can be approximated as a row of cylinders (Fig. 1A,B). The leakiness (Fig. 1C) of a pair of bristles is defined as the ratio of the volume of fluid that actually moves between a pair of bristles to the volume across which that bristle pair sweeps in a unit of time (Cheer and Koehl, 1987). Cheer and Koehl (1987) mathematically approximated steady-state flow near two bristles in free space by considering the flow around and between a two-dimensional cross-section of a pair of circular cylinders. They discovered that appendages with bristles that operate at Re_b close to 1 are more leaky and rake-like (Fig. 1D), whereas appendages with bristles operating at very low Re_b are paddle-like (Fig. 1E). A transition in leakiness occurs as the Re_b of the bristles or the width of the gap between them changes. This means that the bristles on tiny insect wings could act as both paddles and rakes during different portions of the stroke. The performance of bristled appendages operating at the biological conditions of thrips ($Re_b = 10^{-2}$) would be expected to change as a function of bristle spacing and velocity (Cheer and Koehl, 1987).

Previous work suggests that a single wing with bristles engaged in steady translation or rotation is almost as effective as a solid wing at producing aerodynamic forces (Sunada et al., 2002; Davidi and Weihs, 2012). While these studies suggest that bristles may not

[1]Department of Mathematics, University of North Carolina, Chapel Hill, NC 27599, USA. [2]Department of Biology, University of North Carolina, Chapel Hill, NC 27599, USA. [3]Department of Biomedical Engineering, University of North Carolina, Chapel Hill, NC 27599, USA.

*Author for correspondence (skjohnsn@email.unc.edu)

S.K.J., 0000-0003-1051-9861

A

B

C

V_{leak} V_{sweep}

D Leaky rake

E Solid paddle

F

G/D
Solid ————————————————
   5   ·
  11   ·   ·   ·   ·   ·   ·   ·   ·   ·   ·   ·
  17   ·   ·   ·   ·   ·   ·   ·
          |←——————— C ———————→|

Re_b	Re_c
10^{-1}	14.5
10^{-2}	1.45
10^{-3}	0.145

Fig. 1. Bristles can act like leaky rakes or solid paddles, depending on the biological conditions. (A) A bristled wing can be modeled in two dimensions using a cross-section through the chord of the wing. (B) The row of two-dimensional cylinders can then be modeled performing desired kinematics. (C) Leakiness is the ratio of the volume of viscous fluid that actually moves between a pair of bristles (V_{leak}) to the volume across which that bristle pair sweeps (V_{sweep}) in a unit of time (the volume of fluid that would move between the bristles in an inviscid fluid). (D,E) The bristle-based Reynolds number (Re_b) influences the fluid dynamic behavior of bristles. Bristles at higher Re_b are more leaky (D), while bristles at low Re_b act more like solid paddles (E). (F) For this study, two-dimensional wings with different G/D ratios were compared with solid wings over a range of Re_b.

significantly alter the aerodynamic forces experienced by a single wing during steady translation, the bristles might offer an aerodynamic benefit during wing–wing interactions (i.e. 'clap and fling' – see below).

To improve lift generation, it is thought that many tiny insects clap their wings together at the end of upstroke and fling them apart at the beginning of downstroke in a flight mechanism called clap and fling (Weis-Fogh, 1973). Previous research has also shown that this stroke results in a large attached leading edge vortex on each wing, which leads to larger lift forces (Lighthill, 1973; Maxworthy, 1979; Spedding and Maxworthy, 1986; Lehmann et al., 2005; Miller and Peskin, 2005, 2009; Lehmann and Pick, 2007). However, it is possible that clap and fling may naturally result from an increase in wing stroke amplitude to make up for a decrease in wing area as the size of the insect decreases. Miller and Peskin (2005) showed that very large forces are required to fling insect wings apart, particularly at $Re<20$, the range of the smallest flying insects. They suggested that bristled, flexible wings could reduce the force required to clap the wings together and fling the wings apart (Miller and Peskin, 2009).

If the Re_b and spacing of the bristles are near the transition where the bristled appendage acts either as a solid paddle or as a leaky rake (Cheer and Koehl, 1987), then during clap and fling it could be possible for the wing to preserve lift by acting as a solid plate during the translational part of the stroke and a leaky rake during the fling. Experiments with physical models have shown that leakiness is increased when bristles move near a boundary (Loudon et al., 1994). During the fling, there could be some flow between the wings'

bristles, enhanced by the presence of the other wing, which would reduce the force required to fling the wings apart. This idea is supported by a previous numerical study that showed that porous wings, compared with solid wings, reduce the drag required to fling two wings apart (Santhanakrishnan et al., 2014). However, it is unclear whether a bristled wing can be treated as a homogenized porous layer and, if so, what the biologically reasonable permeability should be.

The goals of this study were to (1) collect morphological data on the bristles of small insects and (2) investigate whether bristled wings could reduce the force required to fling the wings apart during clap and fling while still maintaining lift during translation. The challenge of studying the fluid dynamics of bristles was in resolving the fluid flow between the bristles near Reynolds numbers of 1. To accurately model the flow between the bristles, a very high grid resolution was required. The effects of Reynolds number, angle of attack, bristle spacing and wing–wing interactions are quantified for biologically relevant parameter values.

MATERIALS AND METHODS
Subjects
Morphological data on 23 species from the family Mymaridae were collected using previously published (see Table S1) high-quality images of insect wings (Melika and Thuroczy, 2002; Huber et al., 2006, 2008; Huber and Baquero, 2007; Lin et al., 2007; Huber and Noyes, 2013). To be used in our study, we required that the images include a scale bar and that the diameter of the bristles at their base

was at least 6 pixels. The body lengths of the insects were previously reported, and are shown again here. While long bristles appear in many insect orders and families, we limited this study to Mymaridae for the following reasons: (1) Mymaridae include the smallest species of winged insects that have been discovered to date; (2) high-quality photographs of many species of Mymaridae are readily available; and (3) by limiting this study to a single family of insects, we minimized phylogenetic effects.
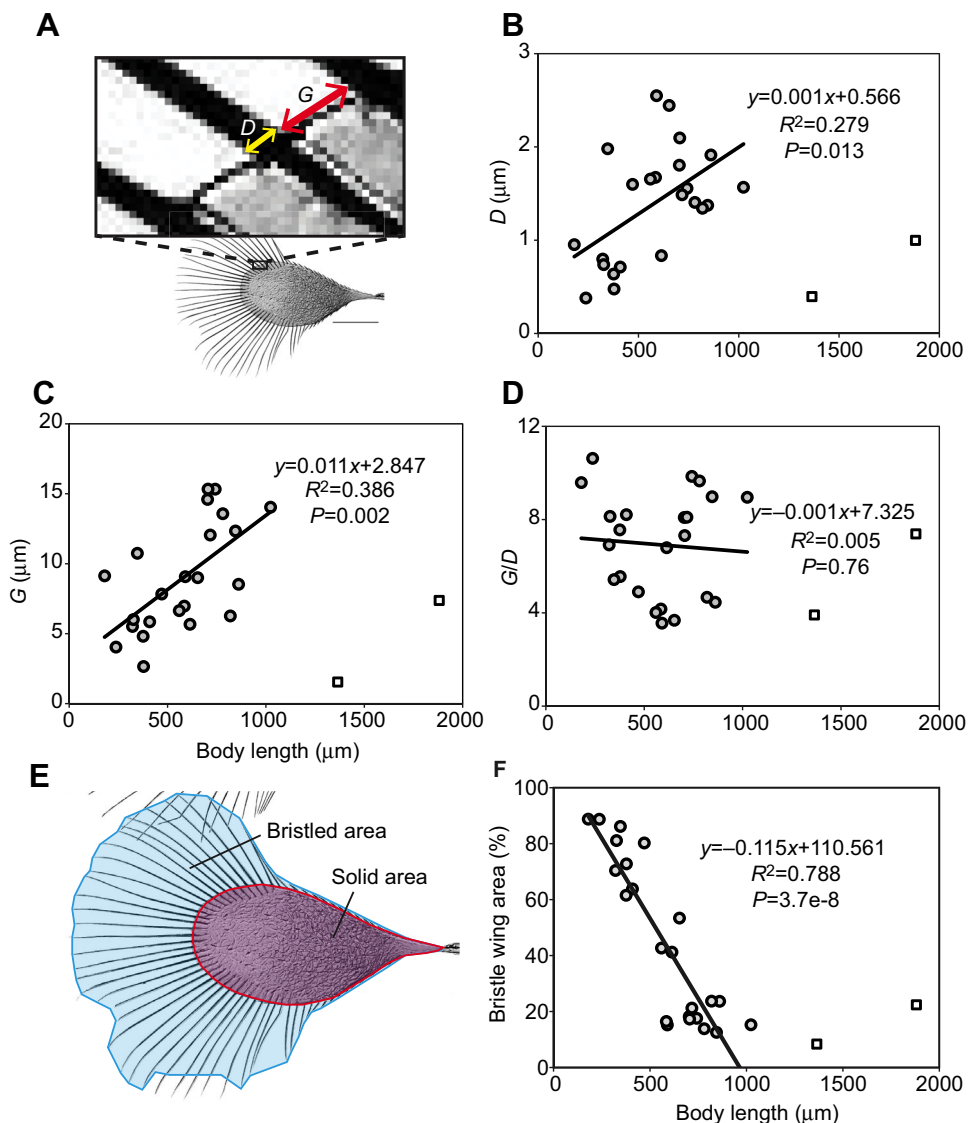
Measurement of bristle morphology

Morphological data were extracted from bristled wing images using ImageJ (Schneider et al., 2012). The images were calibrated using the known length of the scale bar. For each species, a single wing (forewing) was analyzed. The diameter and the gap between bristles (Fig. 2A) were measured along the entire perimeter of the wing at both the base and the tip of the bristles. For each insect species, the gap between bristles varied no more than 10% from the average along the perimeter of the wing. Across all species, the average gap at the tip of the bristles was no more than 10% greater than the average gap at the base of the bristles. The reported diameter and gap values are the average of the base and the tip for the entire wing. The area of the solid portion of the wing and the area of the bristled

portion of the wing were also analyzed (Fig. 2E). Here, we report bristle diameter D, gap between bristles G, gap to diameter ratio G/D, and percentage of wing area that is bristled. We expected the morphological measurements to vary with body length. For each morphological variable, a linear regression analysis was performed and a P-value is reported in Fig. 2 (N=23).

Modeling bristles in 2D

A very fine fluid grid is required to resolve the fluid flow between bristles, making a three-dimensional study computationally challenging. For that reason, we performed our study in two dimensions. An insect wing stroke is commonly approximated in two dimensions using a cross-section through the chord of the wing. Similarly, a row of bristles on an insect wing can be modeled in two dimensions by taking a cross-section through the bristles (Fig. 1A). The resulting row of two-dimensional cylinders can then be moved to perform desired kinematics (Fig. 1B), and the resulting forces and flow structures can be quantified. It is important to note that the bristles are modeled as an array of cylinders that are parallel to the long axis of the wing. The actual wings have bristles that point forward and backward, in addition to pointing laterally at the tip. Our choice allows for the motion to happen in the plane. In this

Fig. 2. Morphological measurements of bristles as functions of body length. (A) The bristle diameter, D (yellow arrow) and the gap between bristles, G (red arrow), were measured for 23 species of Mymaridae. Average values for D (B), G (C) and G/D ratio (D) of a single wing are reported as a function of the average body length of each species. A linear regression was performed and the R^2- and P-values are reported (N=23). (E) The surface area of the wing occupied by bristles was compared with the total area of the wing (solid area+bristled area) to determine the percentage of the wing covered by bristles (F). (Wing shown: forewing of *Mymaromella pala*, holotype; Huber et al., 2008.)

study, bristles were modeled as rows of two-dimensional cylinders. Bristled wings with three different G/D ratios were compared with each other and with a solid wing (Fig. 1F). The G/D ratios were 5:1, 11:1 and 17:1, and the number of bristles per wing was 25, 13 and 9, respectively. These G/D ratios were selected because they capture the range commonly observed in tiny flying insects (approximately 4–12). The number of bristles per wing was selected to allow for the total chord length of the wing, c, to remain constant at 145 bristle diameters. In this way, the chord-based Reynolds number, Re_c, was identical for all of the wings, regardless of G/D.

Chord-based and bristle-based Reynolds numbers

For this study, it was important to differentiate the bristle-based Reynolds number (Re_b) and the chord-based Reynolds number (Re_c). Re_b and Re_c were each defined using Eqn 1. The characteristic length was the diameter of the bristle, D, for Re_b; and the total length of the chord, c, was the characteristic length for Re_c. In the simulations, U was defined as the steady-state velocity of the chord reached after an initial acceleration period. Re_b has been reported for very few species of small insects. It has been estimated that $Re_b=10^{-2}$ ($Re_c\approx10$) for thrips (Ellington, 1975) and $Re_b=10^{-1}$ ($Re_c\approx10$) for *Encarsia formosa* (Kuethe, 1975). For this study, Re_b was varied from 10^{-1} to 10^{-3}. Because the total chord length of the wing remained constant at $145D$, Re_c was 145 times larger than Re_b (see Fig. 1F). The Re_b values most relevant to tiny insects are 10^{-1} and 10^{-2}, which correspond to Re_c of 14.5 and 1.45, respectively. While $Re_c=1.45$ is slightly lower than that observed biologically, these Re_c values are of the order of magnitude relevant to tiny insect flight. Because a Re_b estimate for Mymaridae (which was used in the morphological study) is not available, we draw comparisons to the case most relevant to thrips ($Re_b=10^{-2}$ and $G/D=11$) throughout the Results section.

Leakiness

The leakiness (Fig. 1C) of a pair of bristles was defined as the ratio of the volume of fluid that actually moves between a pair of bristles to the volume across which that bristle pair sweeps in a unit of time (Cheer and Koehl, 1987):

$$\text{Leakiness} = \frac{V_{\text{leak}}}{V_{\text{sweep}}}, \tag{2}$$

where V_{leak} is the volume of fluid that actually moves between two cylinders and V_{sweep} is the volume across which the cylinders sweep. We used VisIt (Childs, 2013) to analyze the flow fields and determine the leakiness from numerical simulations.

Dimensionless drag

To compare the forces from the computations, instantaneous forces experienced by the wings were non-dimensionalized by $0.5\rho U^2 L$, where U is the characteristic steady-state velocity and L is the characteristic length and depended on the application. For simulations with only two bristles, L was the bristle diameter, D, and the reported force was that for each individual bristle. For simulations with full-length wings, L was the chord length, c, and the reported force was the sum of the forces experienced by the entire row of bristles. C_L and C_D denote the lift and drag coefficients, respectively.

Numerical method

We used the immersed boundary method (Peskin, 2002; Griffith et al., 2007; Battista et al., 2015) to model two-dimensional bristles

immersed in a viscous, incompressible fluid. The basic steps of the immersed boundary method for each time step are: (1) calculate the structural forces, with respect to a body coordinate system, generated by the immersed body – in this study, these forces act to impose the wing motion; (2) convert those forces into physical coordinates using a discretized integral transform with a regularized Dirac delta function kernel; (3) solve a common momentum equation for both the fluid and structure, which takes the form of the incompressible Navier–Stokes equations, to determine the velocity of both the fluid and the structure; (4) evaluate the velocity field on the immersed body using a discretized integral transform with a regularized Dirac delta function kernel; and (5) advance to the next time step.

In this study, we used a hybrid finite difference/finite element version of the immersed boundary method (IB/FE). More details on the method can be found in Griffith and Luo (2012) and Jones (2016). The finite element bristle meshes were constructed using Gmsh (Geuzaine and Remacle, 2009), and each individual bristle consisted of at least 16 triangular elements. We confirmed that a single immersed boundary point interacted with the fluid like a sphere with radius of 1.5 grid cells (Bringley and Peskin, 2008), and decreased the bristle radius to compensate for this effective added radius. The computational domain was 500 bristle diameters wide and high, and the bristles were at least 100 bristle diameters from the edges of the computational domain.

We used IBAMR, a software library for immersed boundary simulations with adaptive mesh refinement (Griffith et al., 2007), for all of the fluid dynamic simulations. The adaptive method used four grid levels to discretize the Eulerian equations with a refinement ratio of four between levels. Regions of fluid that were close to the bristles or whose vorticity was above $0.125\ \text{s}^{-1}$ were discretized at the highest level of refinement. The boundary conditions were set to no-slip (fluid velocity, $\mathbf{u}=0$) on all sides of the computational domain. The bristles were moved using a preferred position that was changed in time. A penalty force was applied proportional to the distance between the actual and desired boundary positions.

Changes in spacing between neighboring bristles have the most pronounced effect at Re_b approaching 1 and when the bristles are already fairly close together (Cheer and Koehl, 1987). For that reason, we performed a grid refinement study focused on two bristles with $Re_b=10^{-1}$ (the largest Re_b used in this study) and a G/D ratio of 5:1 (the smallest spacing used in this study). The average percentage difference in leakiness between a 2048×2048 discretization and a 4096×4096 discretization was less than 3% ($G/D=5$, $Re_b=10^{-1}$). For computational efficiency, effective 2048×2048 discretization was used for all other simulations in this study. Other simulation-specific numerical parameters are listed in Table S2.

Validation of the numerical method

The simulation code used in this paper has been validated for standard fluid structure interaction problems (Griffith et al., 2007; Griffith and Luo, 2012). In addition to performing the above convergence study, we wanted to further validate our model by comparing the results of the model with those from a previously published analytical model given by Cheer and Koehl (1987). In the model by Cheer and Koehl (1987), the drag acting on the bristles and leakiness between two two-dimensional bristles were determined analytically. To compare the numerical model with the previously published analytical model, we simulated two bristles translating at a steady velocity over a range of Re_b (Fig. 3A). At lower Re_b, a large region of fluid was moved with the bristles, and

the bristles acted more like a solid plate. At larger Re_b, the bristles entrained a smaller region of fluid, and the bristles were leakier. For example, at $Re_b=10^{-3}$, the region around the bristles looked like a uniform flow field, whereas at $Re_b=0.5$, the direction of flow quickly changed over a short distance from the bristles.

The leakiness and forces (Fig. 3B,C) of the numerical simulation were compared with Cheer and Koehl's (1987) analytical solution over a range of Re_b. The reported leakiness and drag are for bristles in fully developed flow (i.e. steady state). We defined steady state as less than a 1% change in leakiness or force per unit of dimensionless time. Overall, there was good agreement between the IBAMR simulations and the analytical model by Cheer and Koehl (1987). The differences that do exist are likely due to the different boundary conditions used in the numerical and analytical models. In the numerical model, the no-slip condition was used at the boundary, introducing some wall effects at lower Re_b, whereas the analytical model assumed an infinite domain. This explains why the numerical model was leakier and experienced greater forces than the analytical model at lower Re_b. Differences at higher Re_b may result from the use of the Oseen approximation in the analytical model, which is only appropriate for a certain range of Re.

RESULTS
Bristle morphology
The bristle diameter D, gap between bristles G, gap to diameter ratio G/D, and percentage of wing area that is bristled are shown as functions of body length (Fig. 2). In general, the bristle diameter and the gap between bristles increased as the size of the insect increased (Fig. 2B,C). There was no correlation, however, between the gap to diameter ratio and the body length of the insect (Fig. 2D). There was a very strong correlation between the surface area of the wing occupied by bristles and the body length of the insect (Fig. 2F). As the insect body length decreased, the percentage of the wing surface area occupied by bristles increased.

Bristles and angle of attack
We expected the performance of bristles to change with the angle of the wing relative to the approaching flow (e.g. the angle of attack). While studying flow between gill rakers, Cheer et al. (2012) discovered that the speed and approaching angle of the flow play a role in generating vortices that reduce the effective size of the gap between rakers. This resulted in changes in the effective leakiness. While these results were obtained at $Re_b=37.5$ to 225,
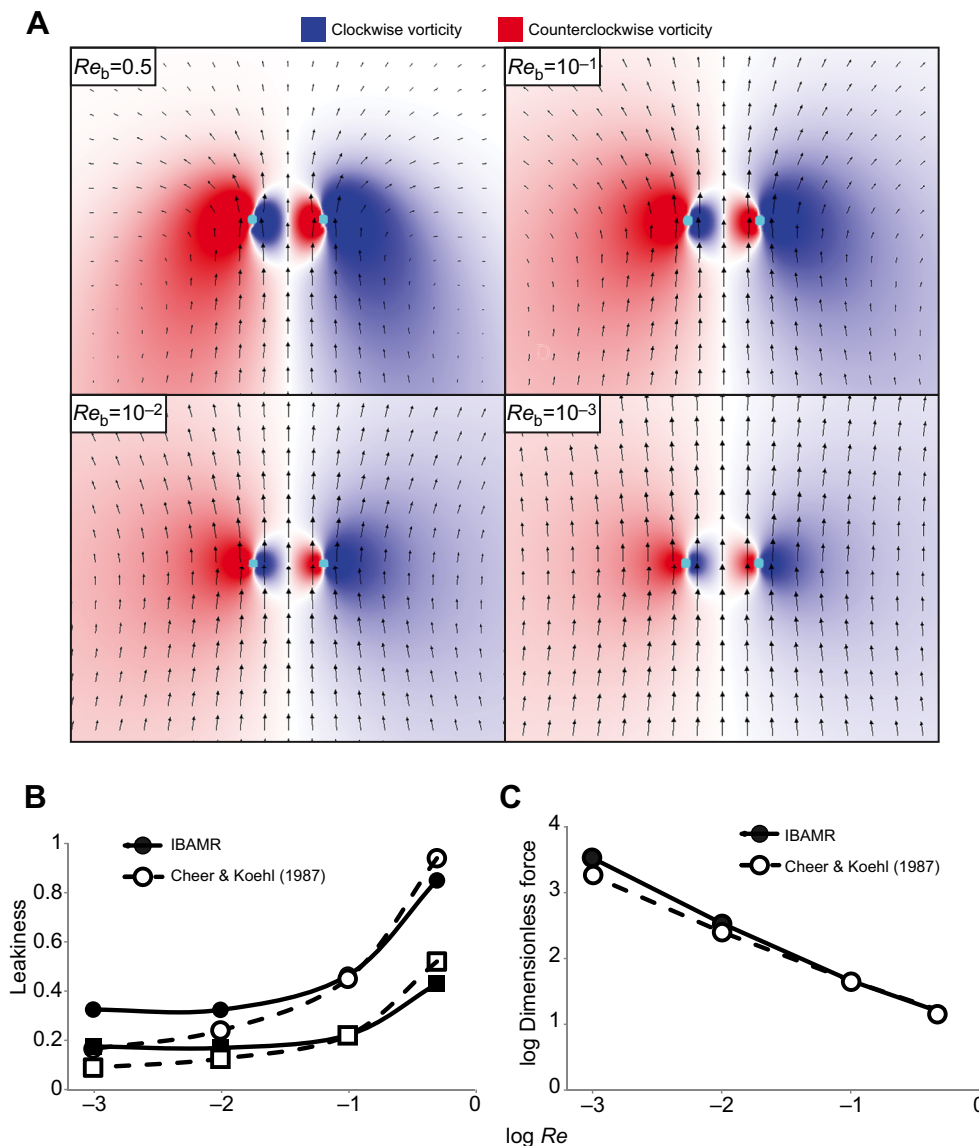
Fig. 3. Validation of the numerical model. (A) Vorticity plots of two bristles (light blue) translating at $Re_b=0.5$, $Re_b=10^{-1}$, $Re_b=10^{-2}$ and $Re_b=10^{-3}$ ($G/D=5$). The frame shown is at steady state, after the bristles have traveled $150D$ (the bristles are moving toward the top of the page at a constant velocity). The vectors show the direction of flow and are scaled to the magnitude of the flow velocity (minimum=0, maximum=0.2). The color map shows the vorticity of the fluid (minimum=−30 and maximum=30). (B,C) Comparison of the numerical method (IBAMR) and a previously published analytical model of 2 bristles (Cheer and Koehl, 1987). (B) Leakiness as a function of Re_b for a G/D ratio of 5:1 (squares) and 15:1 (circles) for the two different methods. (C) The log of the drag coefficient plotted versus the log of Re_b. The data from IBAMR are for a G/D ratio of 5:1. The data from Cheer and Koehl (1987) are for a 0.1 μm cylinder with a neighbor 0.3 μm away.

we expected to see a similar change in leakiness with angle of attack at lower Re_b.

Flow visualization of the entire bristled wing revealed differences between the different G/D ratios (Fig. 4A). Vector fields are shown for a solid wing and for bristled wings with the three G/D ratios translating at an angle of attack of 45 deg. These results show that significantly more fluid was entrained by the solid wing and wings at lower G/D ratios. The leading edge vortex was slightly more diffuse at G/D=17 than at G/D=5, which might explain the slightly larger lift to drag ratio at G/D=5, described below.

To investigate the effect of angle of attack on bristle performance, we compared the lift and drag experienced by a single wing translating (Fig. 1B,C) at the relevant Re_b of thrips ($Re_b=10^{-2}$, $Re_c=1.45$). The angle of attack of the row of bristles ranged from 0 to 90 deg, and the row translated at a steady velocity until each wing traveled 150 bristle diameters (approximately one wing length). The reported force was the sum of the forces experienced by the entire row of bristles, normalized by the chord length.

For all angles of attack, the magnitude of the force coefficients decreased with increasing G/D ratios (Fig. 4B,C). The magnitude of this effect was greatest for lift at angles of attack near 45 deg (Fig. 4B), and for drag at angles of attack approaching 90 deg

(Fig. 4C). Interestingly, the effect of G/D was greater at higher angles of attack than at lower angles of attack. For example, at an angle of attack of 9 deg, there was little difference in lift between the three bristled wings, whereas at an angle of attack of 81 deg, there was a noticeable increase in lift as G/D decreased. Similarly, there was a smaller difference in drag at lower angles of attack, whereas there was a large increase in drag with decreasing G/D at higher angles of attack. This was most likely because lower angles of attack reduced the effective size of the gap between bristles, leading to changes in leakiness and forces (Cheer et al., 2012).

Although the lift and drag experienced by a bristled wing were affected by changes in G/D, the value of G/D appeared to have little effect on the lift to drag ratio (Fig. 4D) Specifically, in these simulations, there was no difference in C_L/C_D for angles of attack <27 deg. At angles of attack >27 deg, there appeared to be no difference between G/D=5 and G/D=11, and G/D=17 performed only slightly below the other two.

The effect of angle of attack on bristle performance was particularly evident in the aerodynamic polars of the average coefficients of lift and drag shown in Fig. 4E. While the G/D ratio affected C_L and C_D at higher angles of attack, it appeared to have less influence on C_L and C_D at lower angles of attack.
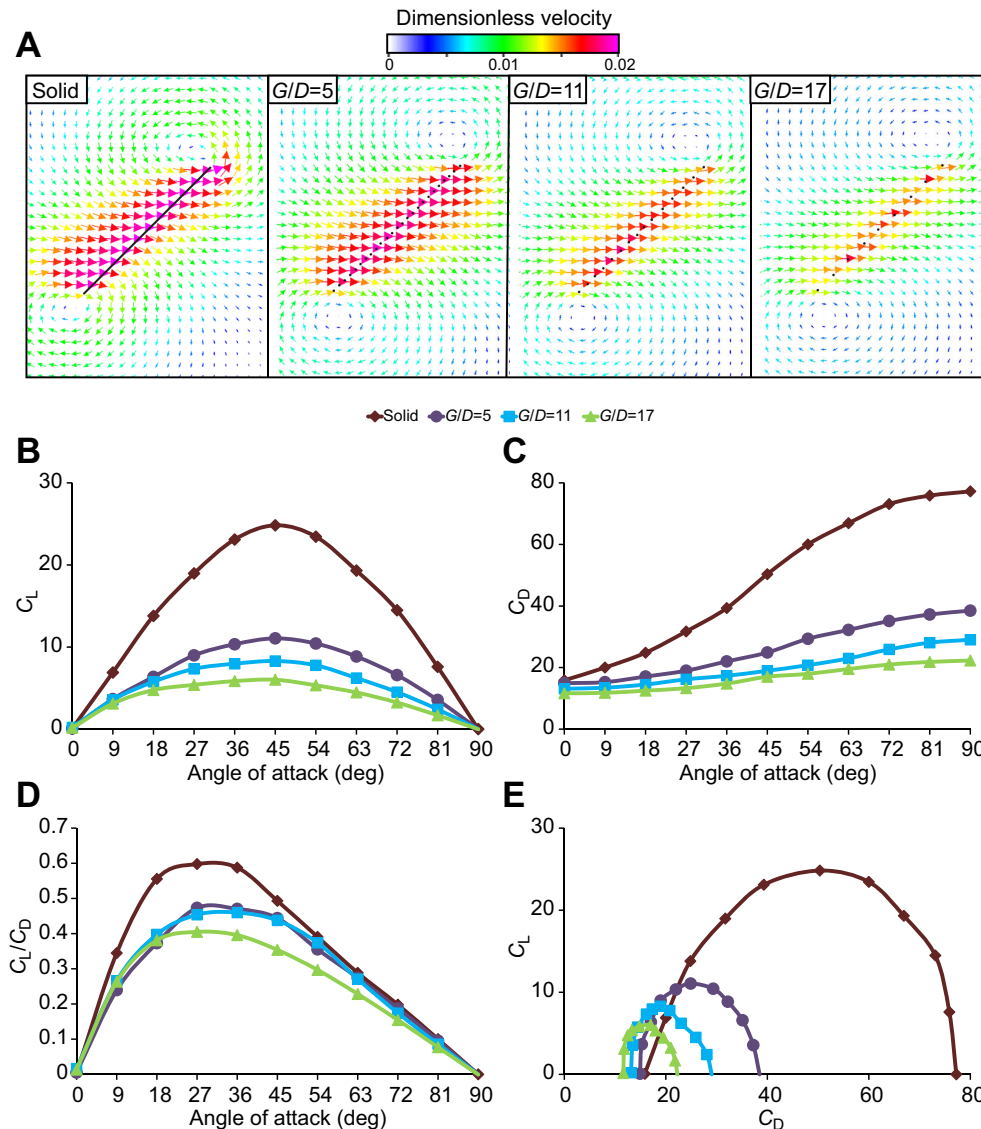
Fig. 4. Aerodynamic performance of a row of bristles translating at an angle of attack of 45 deg. (A) Vorticity plots comparing a solid wing and bristled wings translating at an angle of attack of 45 deg and $Re_b=10^{-2}$ (chord-based Reynolds number, $Re_c=1.45$). The wings are moving to the right. The frame shown is at steady state, after the bristles have traveled 150D (approximately 1 wing length). The wing is traveling at a dimensionless velocity of 0.02. The vectors show the direction of flow and the color is scaled to the magnitude of the flow velocity (minimum=0, maximum=0.02). (B,C) Dimensionless steady-state lift (C_L, B) and drag (C_D, C) coefficients experienced by a bristled wing translating at steady state over a range of angles of attack ($Re_b=10^{-2}$, $Re_c=1.45$). (D) The aerodynamic polars of the average C_L/C_D ratio over a range of angles of attack and (E) C_L versus C_D for three different G/D ratios.

Vorticity plots (Fig. 5) of the leading edges of the row of bristles at angles of attack of 18, 45 and 72 deg showed differences in the fluid behavior as the angle of attack changed. Each translating bristle generated a pair of oppositely spinning attached vortices. The magnitude and size of these vortices were greater near the leading and trailing edges of the wing, and smaller near the center of the wing. With decreasing angle of attack, the vortices became more diffuse and extended over a greater area, effectively reducing the size of the gap between bristles (see Fig. 5A). While studying flow between gill rakers, Cheer et al. (2012) discovered a similar relationship between angle of the flow and the effective size of the gap between rakers, leading to changes in leakiness. This suggests that at lower angles of attack, bristled wings may act more like solid wings than they do at higher angles of attack.

Wing–wing interactions

To investigate the effect of wing–wing interactions (Fig. 6), we compared a single wing with a pair of wings moving apart. We investigated both pure wing translation and pure wing rotation for bristled and solid pairs of wings (see Fig. 1F) at Re_b ranging from 10^{-1} to 10^{-3} (Re_c ranging from 14.5 to 0.145). The wing length, L, was defined as the length of the row of bristles and was constant across all G/D ratios.

In the case of two wings translating apart (Fig. 6A), the wings started at a distance of $0.1c$, where c is the chord length of the wing, based on observations of clap and fling in thrips (Santhanakrishnan et al., 2014). They accelerated over a distance of $0.05c$, then translated at a steady-state velocity until each wing had traveled $0.8c$, so that the two wings were $2c$ apart at the end of the simulation. For a single wing translating, the wing performed the exact same kinematics, without the presence of a second wing.

In the case of two wings rotating apart (Fig. 6B), the wing rotated about the trailing edge, as is commonly seen in fling. The velocity and distance traveled were based on the leading edge of the wing. Similar to translation, the wings started at a distance of $0.1c$. They accelerated apart until the wing tips had traveled $0.05c$, then rotated at a steady velocity until the wings tips had each traveled $1c$. For a single wing rotating, the wing performed the exact same kinematics, without the presence of a second wing. Re_b was based on the wing tip velocity.

In all cases, the drag required to translate (Fig. 6C) or rotate (Fig. 6D) two wings apart was greater than the drag required to move a single wing. The peak drag experienced for two wings performing a 'fling' was much greater than the peak drag experienced by a single wing. This was particularly true at lower Re_b and smaller G/D ratios. For example, there was a 28-fold increase in the maximum drag required to translate two solid wings versus one solid wing at $Re_b=10^{-3}$, whereas there was only a 5-fold increase in the maximum drag at $Re_b=10^{-1}$. In contrast, there was a 4-fold increase in the drag required to translate two bristled wings versus one bristled wing at $Re_b=10^{-3}$ and $G/D=17$, whereas there was only a 0.1-fold increase in the drag required at $Re_b=10^{-1}$. At the biological conditions most relevant to thrips ($Re_b=10^{-2}$ and $G/D=11$), there was only a 2-fold increase in the drag required to translate two bristled wings versus one bristled wing, compared with a 10-fold increase for a solid wing at the same Re_b.

A more careful inspection of the drag as a function of time as two wings translate apart (Fig. 7) reveals more details about the effect of bristles in wing–wing interactions. In all cases, the drag peaked as the wings accelerated at the beginning of the stroke, then the drag plateaued to a steady state. In all cases, two wings experienced greater drag than a single wing. In particular, the magnitude of the peak was much larger in the presence of a second wing. As the
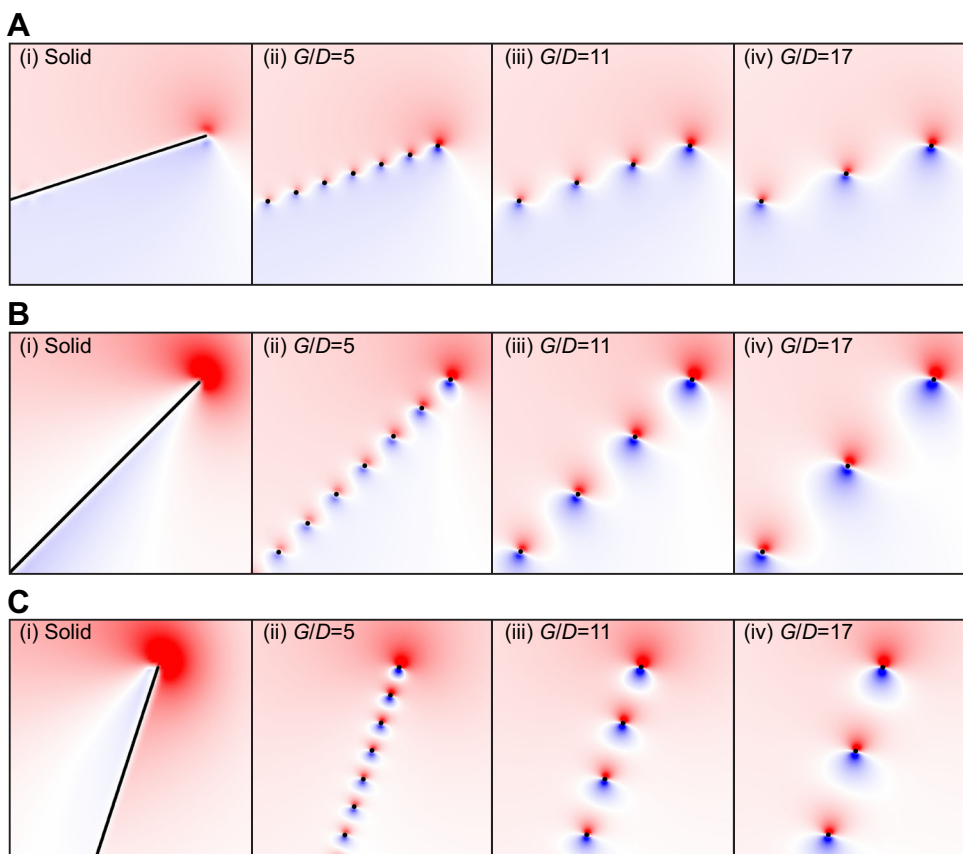
Fig. 5. Vorticity plots of the leading edge of a row of bristles. The bristles are translating at an angle of attack of (A) 18 deg, (B) 45 deg and (C) 72 deg. A solid wing (i) is compared with bristled wings with three G/D ratios: 5 (ii), 11 (iii) and 17 (iv). The row of bristles is moving to the right, and has reached steady state ($Re_b=10^{-2}$, $Re_c=1.45$). Only the leading edge of the row is shown. The color map shows the vorticity of the fluid (minimum=−5 and maximum=5; red, counterclockwise rotation; blue, clockwise rotation).
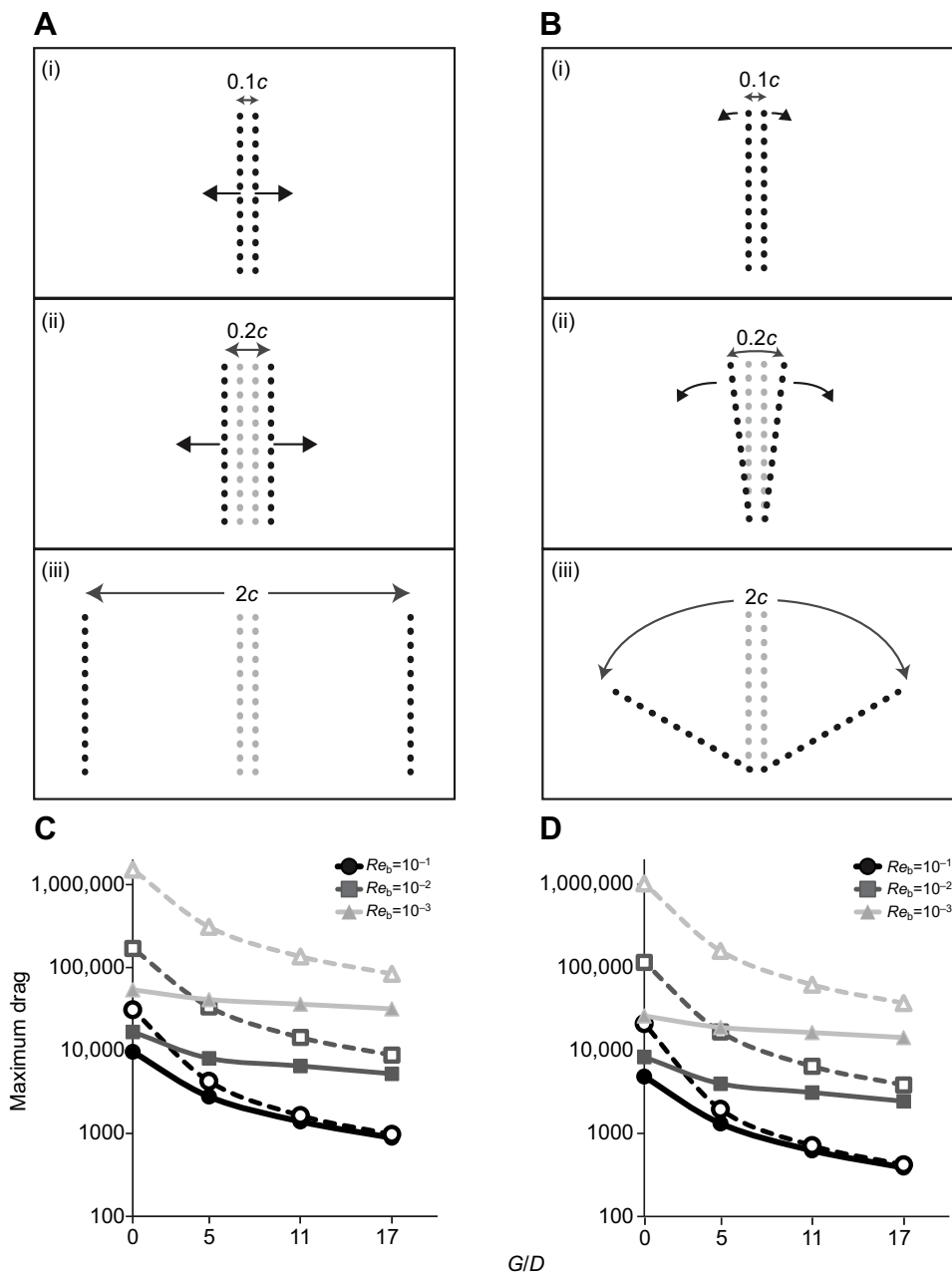
Fig. 6. Wing–wing interactions.
(A,B) Illustration of bristled wing–wing interactions. A row of bristles can translate (A) or rotate apart (B). In the numerical simulations, the bristled wings start a distance of 0.1c apart (i). They accelerate until they are 0.2c apart (ii), and then translate or rotate at a steady velocity until they are 2c apart (iii). In the case of a translating wing (A), the angle of attack is 90 deg. In the case of a rotating wing (B), the wing rotates about the trailing edge. Velocity and distance traveled are based on the leading edge. Numerical simulations of a single wing perform the exact same kinematics in the absence of a second wing. (C,D) Maximum dimensionless drag for translation (C) and rotation (D) experienced by 1 wing (solid symbols) or 2 wings interacting (open symbols) at Re_b=10^{-1} (Re_c=14.5), Re_b=10^{-2} (Re_c=1.45) and Re_b=10^{-3} (Re_c=0.145). The maximum drag is the peak drag experienced by a single wing translating or the drag experienced by an individual wing that is part of a pair moving apart.

wings continued to move farther apart, however, the drag decreased and approached that of a single wing. The increase in drag in the presence of a second wing was dependent upon Re_b and G/D. The magnitude of the effect increased with decreasing Re_b and decreasing G/D ratio. At the conditions most relevant to thrips (Re_b=10^{-2} and G/D=11), there was little difference in drag due to the presence of a second wing after the wings traveled 0.5 wing lengths (Fig. 7B). A similar pattern was seen for the drag of two wings rotating (not shown). In the case of two wings translating apart (Fig. 6A), the wings do not produce any lift. However, we show lift as a function of time for the case of two wings rotating apart in Fig. S1. Like drag, lift was reduced by bristles compared with a solid wing, and this effect was even more pronounced in the presence of a second wing.

Velocity vectors of the fluid around the leading edge of two wings moving apart and a single wing translating are shown for Re_b=10^{-1}, 10^{-2} and 10^{-3} in Figs 8, 9 and 10, respectively. In general, the bristles were leakier as Re_b increased and as G/D increased. The leakiness of the bristles was enhanced by the presence of a second wing. There were fewer differences in the flow between a single wing and two wings as Re_b increased and G/D increased. For example, at Re_b=10^{-1} and G/D=17, the fluid fields were very similar between a single wing (Fig. 8Ai) and two wings (Fig. 8Bi). There was also little difference in the forces experienced in these two cases (Fig. 6C and Fig. 7A). In both cases, there was fluid flow between bristles in the direction opposite to motion. The magnitude of this fluid flow was greater in the presence of a second wing (Fig. 8B). As G/D decreased, however, less fluid was able to flow between bristles.

As Re_b decreased, differences between one and two wings became more apparent. At Re_b=10^{-2} and Re_b=10^{-3}, there was a visible difference in the amount of fluid that traveled with a single wing translating (Figs 9A, 10A) compared with two wings moving apart (Figs 9B, 10B). The presence of a second wing enhanced
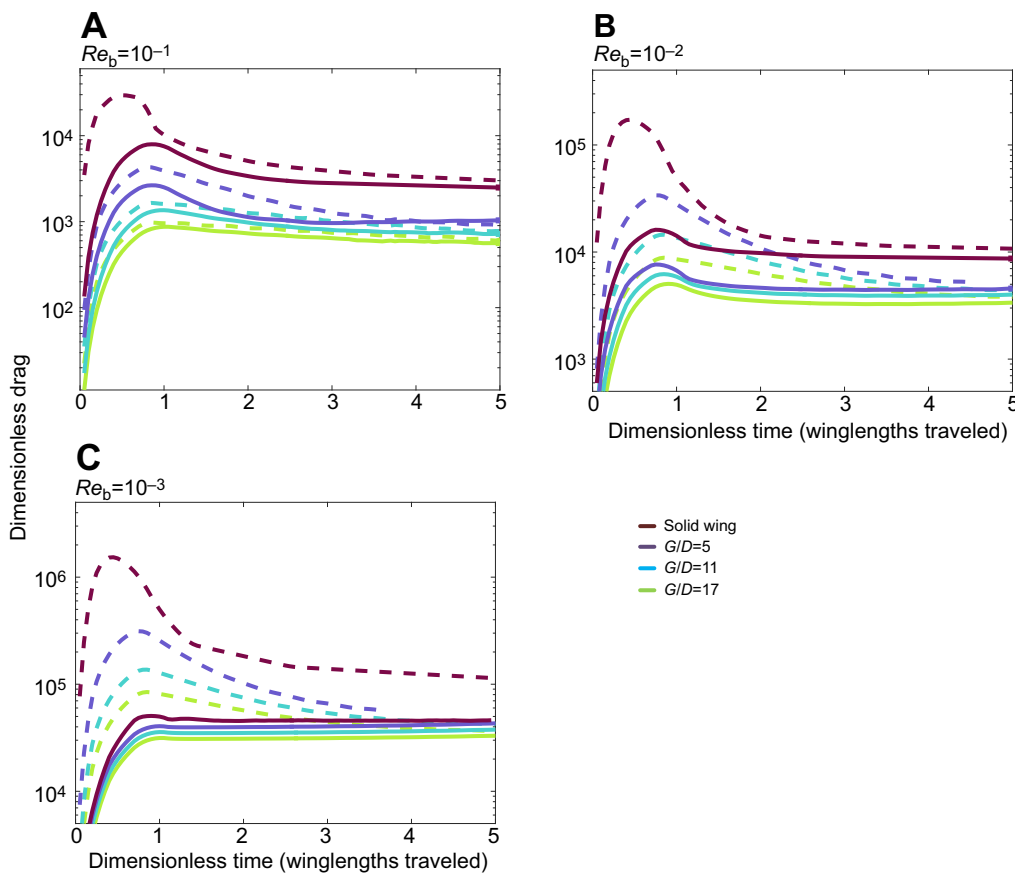
Fig. 7. Instantaneous dimensionless drag as a function of dimensionless time at different Re_b. (A) $Re_b=10^{-1}$ ($Re_c=14.5$), (B) $Re_b=10^{-2}$ ($Re_c=1.45$) and (C) $Re_b=10^{-3}$ ($Re_c=0.145$). A single wing translating (solid lines) is compared with two wings performing a 'fling' (dashed lines) for three different bristle G/D ratios and a solid wing (angle of attack=90 deg). Only the first 0.75 wing lengths traveled are shown.

the flow between bristles, especially at lower Re_b. For example, in the presence of a second wing, fluid flowed between bristles in the direction opposite to motion when $G/D=17$ (Figs 9Bi, 10Bi), whereas fluid moved in the direction of motion between bristles in the absence of a second wing (Figs 9Ai, 10Ai).

DISCUSSION
In this study, we found that: (1) as the body length of Mymaridae decreased, the diameter and gap between bristles decreased; (2) as the body length of Mymaridae decreased, the percentage of the wing surface area covered by bristles increased; (3) the decrease in force with increasing G/D ratio is greater at higher angles of attack than at lower angles of attack, suggesting that bristled wings may act more like solid wings at lower angles of attack than they do at higher angles of attack; (4) in wing–wing interactions, an increase in drag in the presence of a second wing is Re_b and G/D ratio dependent – the magnitude of the effect increased with decreasing Re_b and decreasing G/D ratio; and (5) bristled wings significantly decrease the drag required to fling two wings apart compared with solid wings, especially at lower Re_b. Regarding the last point, it is important to note that the horizontal force required to fling the wings apart can be an order of magnitude greater than the force required to translate a single wing (Miller and Peskin, 2009; Santhanakrishnan et al., 2014). As the wings move in opposite directions at the beginning of the fling, these forces cancel. Although lift is reduced with bristled wings during the fling, peak drag is dramatically reduced. We propose that bristles lower the substantial force required to peel wings apart at low Re.

The results of our morphological study reveal that bristles occupy a greater percentage of the surface area of the wings of Mymaridae as the body length of the insects decreases (Fig. 2E). This supports the idea that bristles may play an important physiological or mechanical role for the smallest insects. We also found that the diameter and gap between bristles decreased with body length; however, there was no relationship between the G/D ratio and body length.

Previous work suggests that single translating bristled wings produce almost as much aerodynamic force as solid wings (Sunada et al., 2002; Davidi and Weihs, 2012). Our results show that drag and lift magnitude decrease as the space between bristles increases (Fig. 4B,C), whereas the spacing between bristles appears to have little effect on the lift to drag ratio (Fig. 4D) over a range of Re_b and angles of attack. A previous study of porous wings in single wing translation also showed only a small improvement in the lift to drag ratio for a biologically relevant range (Santhanakrishnan et al., 2014).

Our results support the idea that bristles could offer an aerodynamic benefit during wing–wing interactions. Many tiny insects clap their wings together at the end of upstroke and fling them apart at the beginning of the downstroke using a mechanism known as clap and fling. At the Re_b relevant to tiny insects, very large forces are required to clap the wings together and fling the wings apart (Miller and Peskin, 2005). A computational study by Miller and Peskin (2009) showed that flexibility can reduce the drag required to fling wings apart; however, the drag generated is still 3–5 times (or even more at the lowest Re) greater than a single wing translating at $Re<30$. In addition to flexibility, bristles may help reduce the drag experienced during fling.

For the parameter range considered, bristles significantly decrease drag compared with a solid wing (Fig. 7). For both single wings translating and wings engaged in fling, the results showed that as G/D increased, drag decreased. Bristles more significantly reduced the drag required to fling two wings apart, compared with single wings. For example, at the biological
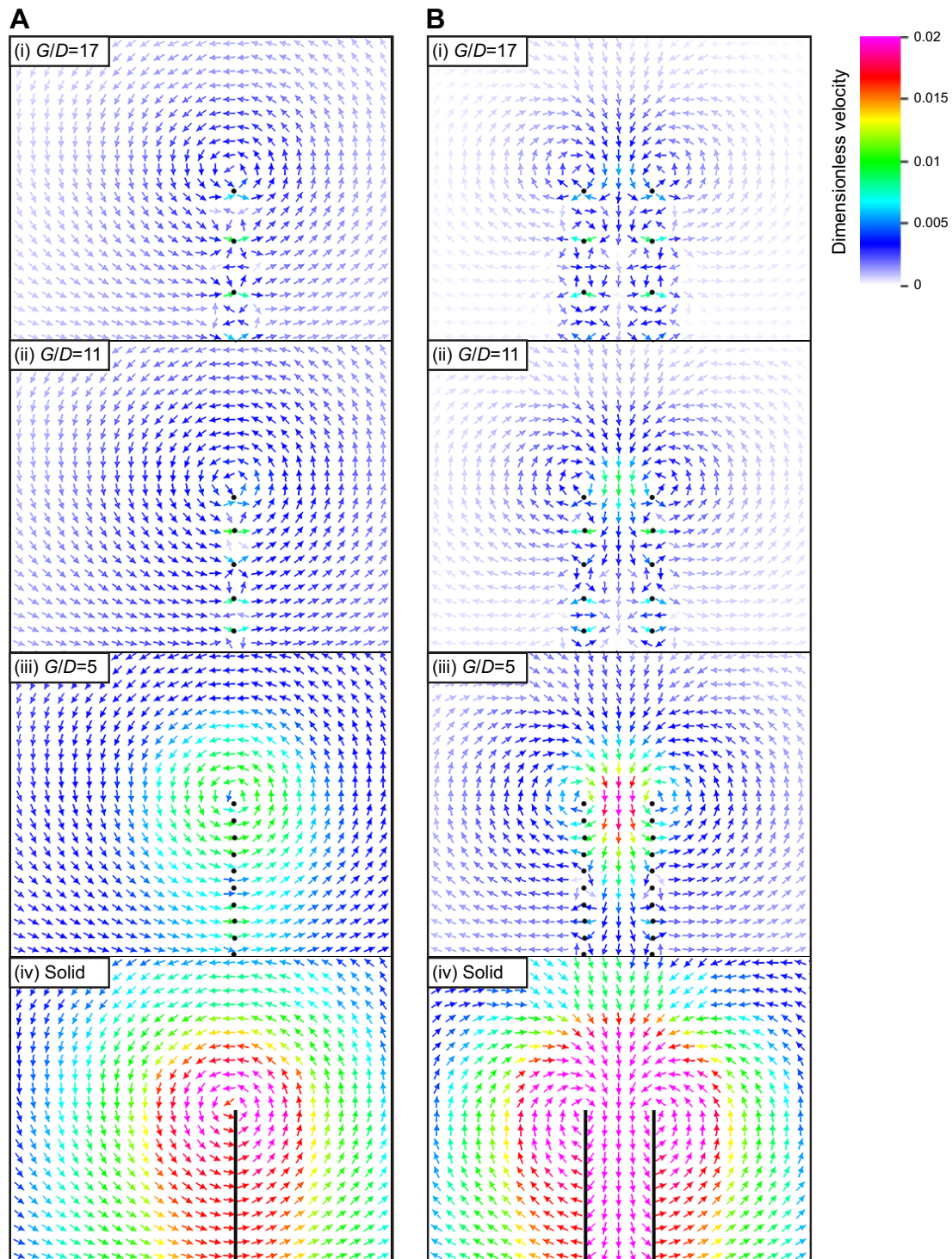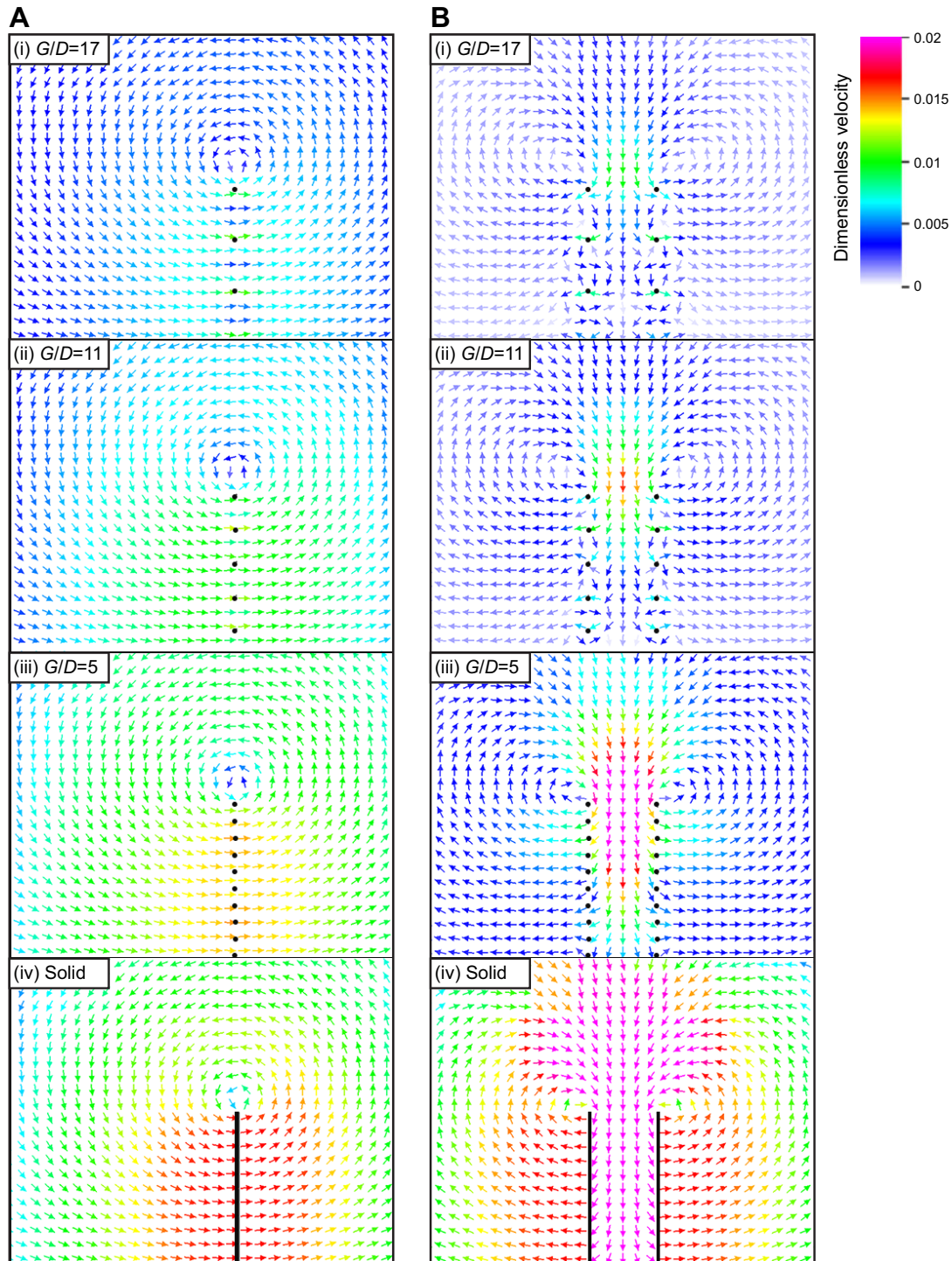
Fig. 8. Velocity vector field plots of the leading edges of a single wing translating to the right and two wings translating apart at $Re_b=10^{-1}$ ($Re_c=14.5$). (A) Single wing; (B) two wings. Wings with G/D ratios of 17 (i), 11 (ii) and 5 (iii), are compared with a solid wing (iv). The frame shown is at the end of acceleration, when the wings are 0.2 wing lengths apart. The vectors show the direction of flow and the color is scaled to the magnitude of the flow velocity (minimum=0, maximum=0.02).

conditions most relevant to thrips ($Re_b=10^{-2}$ and $G/D=11$), the drag required to fling two bristled wings apart was only two times greater than that for a single wing translating, compared with a 10-fold increase in drag for a solid wing at the same Re_b.

Our results reveal important differences between single wings and wing–wing interactions (see Tables S3, S4). At $Re_b=10^{-3}$, a bristled wing with $G/D=5$ experienced 76% of the drag of a solid

wing when engaged in steady translation, whereas a wing engaged in fling experienced only 20% of the drag of a solid wing. At the biological conditions of thrips ($Re_b=10^{-2}$, $G/D=11$), the maximum drag required to fling two solid wings apart was 12 times greater than the drag required to fling two bristled wings apart, whereas the drag during steady translation was only 2.5 times greater for a solid wing than a bristled wing ($Re_b=10^{-2}$, $G/D=11$).
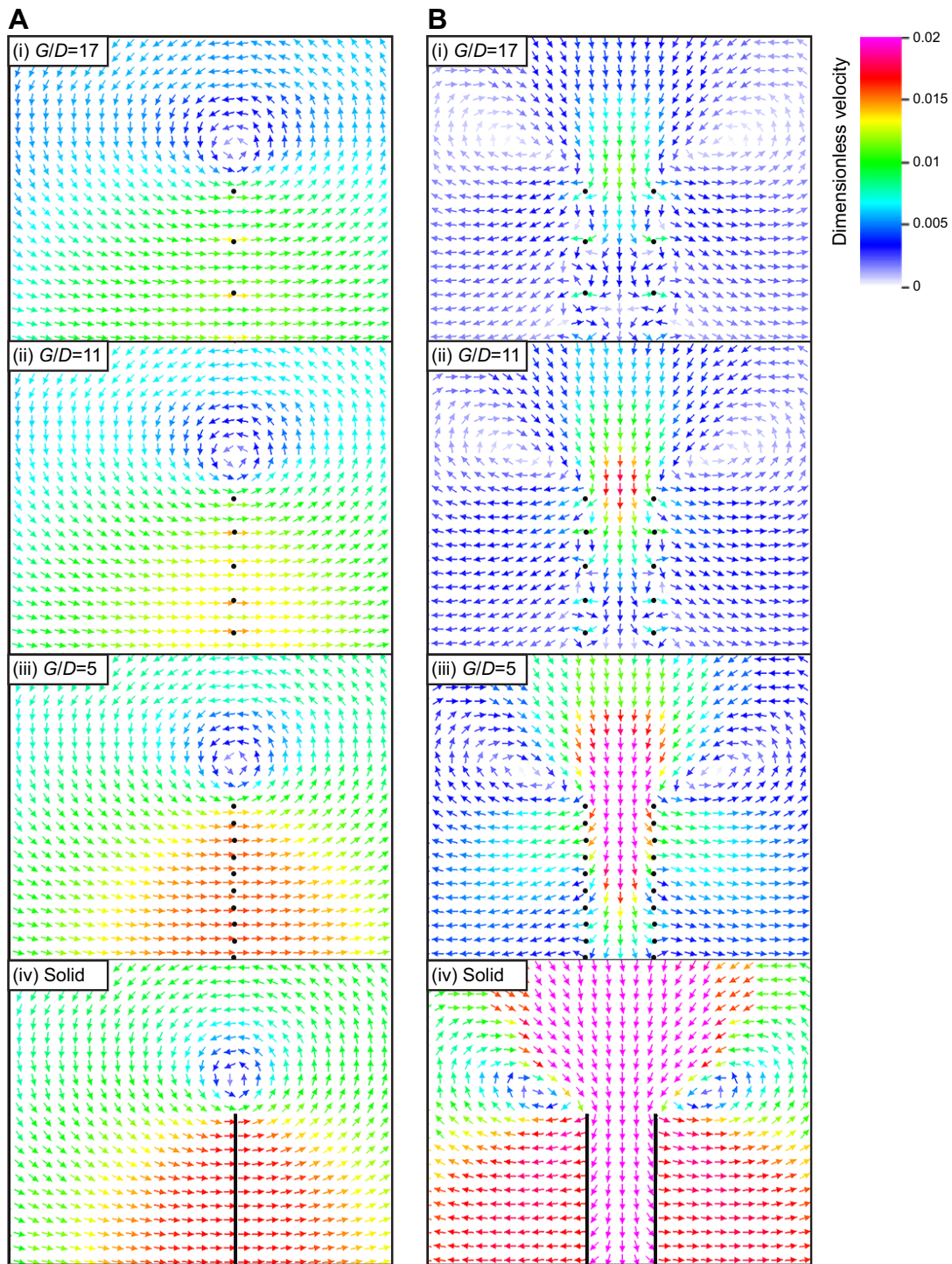
Fig. 9. Velocity vector field plots of the leading edges of a single wing translating to the right and two wings translating apart at $Re_b=10^{-2}$ ($Re_c=1.45$). (A) Single wing; (B) two wings. Wings with G/D ratios of 17 (i), 11 (ii) and 5 (iii) are compared with a solid wing (iv). The frame shown is at the end of acceleration, when the wings are 0.2 wing lengths apart. The vectors show the direction of flow and the color is scaled to the magnitude of the flow velocity (minimum=0, maximum=0.02).

Single bristled wings may act even more like solid plates than is suggested by these results if they are translating at an angle of attack less than 90 deg. Fig. 4B,C shows that the decrease in force with increasing G/D was greater at higher angles of attack than at lower angles of attack, suggesting that bristled wings may act more like solid wings at lower angles of attack than they do at higher angles of attack. Further, the spacing between bristles appeared to

have little effect on the lift to drag ratio (Fig. 4D) for a single wing translating.

In total, these results support the idea that bristles may offer an aerodynamic benefit during clap and fling in tiny insects. The bristles significantly reduce the force required to fling the wings apart, compared with a solid wing. Although this study only considered fling, we expect that bristles have a similar force-

Fig. 10. Velocity vector field plots of the leading edges of a single wing translating to the right and two wings translating apart at $Re_b=10^{-3}$ ($Re_c=0.145$). (A) Single wing; (B) two wings. Wings with G/D ratios of 17 (i), 11 (ii) and 5 (iii) are compared with a solid wing (iv). The frame shown is at the end of acceleration, when the wings are 0.2 wing lengths apart. The vectors show the direction of flow and the color is scaled to the magnitude of the flow velocity (minimum=0, maximum=0.02).

reducing effect during the clap portion of the stroke. The idea that bristles offer an aerodynamic benefit during clap and fling is supported by a numerical study of porous wings, which showed that porous wings, compared with solid wings, reduce the drag required to move two wings apart (Santhanakrishnan et al., 2014). Moreover, bristles reduce the force experienced by a wing to a greater extent during fling than during steady translation. Following fling, the

force approaches that experienced by a single wing. Additionally, it could be possible for the bristled wing to preserve lift by acting more like a solid plate during the translational part of the stroke, especially if the angle of attack is less than 90 deg.

It is important to consider that the bristles may offer other benefits to insects. While we limited our study to the aerodynamics role of bristles, other functions have been suggested. For example, the

bristles might offer an advantage to insects by decreasing their weight (Sunada et al., 2002). The bristles might also enhance electrostatic charges, which has been shown to help in the dispersal of spiders (Gorham, 2013). In thrips, the bristles can spread out to unfold the wing, or collapse to fold the wing (Ellington, 1980), suggesting they may play a role in wing position and area. The role of wing bristles in sensing airflow and wing vibrations has been suggested for fruit flies, moths and other insects (Ai et al., 2010; Ai, 2013), and it is possible the bristles of some tiny insects also serve the same purpose.

Limitations

While this study was conducted using two-dimensional cross-sections of infinitely long bristles, we anticipate that the three-dimensional geometry and finite length of insect wing bristles will play an important role in their leakiness. We expect that the leakiness of bristles in three spatial dimensions would be lower than the leakiness in two dimensions: rather than flowing between bristles, fluid may flow around the bristles. Cheer et al. (2012) demonstrated differences in the leakiness of the lower and upper part of fish rakers, so we may expect leakiness to vary with distance from the solid portion of the wing.

Another limitation to the two-dimensional study is that the bristles are modeled as an array of cylinders that are parallel to the long axis of the wing. The actual wings have bristles that point forward and backward, in addition to pointing laterally at the tip. Similarly, the velocity at the base of the wing will be lower than the velocity at the tip, which will change the leakiness and force.

Finally, the distance between the wings at the start of fling was not varied: the wings started at 0.1 wing lengths apart. Previous work has demonstrated that lift is enhanced as the distance between wings approaches zero (Kolomenskiy et al., 2010, 2011). However, observations of clap and fling in thrips have shown that the distance between the wings at the beginning of fling varies from about 1/4 to 1/10 of the chord length (Santhanakrishnan et al., 2014).

The results of this simple study can be used to generate new questions about small-insect flight and the role of bristles. In particular, small changes in the angle of attack, G/D ratio and Reynolds number can have a large effect on the forces generated at the scale of tiny insects. Three-dimensional studies of a bristled wing would be an important next step to understanding the aerodynamics of bristles.

Supplementary information
Supplementary information available online at
http://jeb.biologists.org/lookup/doi/10.1242/jeb.143362.supplemental

References
Ai, H. (2013). Sensors and sensory processing for airborne vibrations in silk moths and honeybees. *Sensors* **13**, 9344-9363.

Ai, H., Yoshida, A. and Yokohari, F. (2010). Vibration receptive sensilla on the wing margins of the silkworm moth Bombyx mori. *J. Insect Physiol.* **56**, 236-246.

Barta, E. (2011). Motion of slender bodies in unsteady Stokes flow. *J Fluid Mech.* **688**, 66-87.

Barta, E. and Weihs, D. (2006). Creeping flow around a finite row of slender bodies in close proximity. *J. Fluid Mech.* **551**, 1-17.

Battista, N. A., Baird, A. J. and Miller, L. A. (2015). A mathematical model and MATLAB code for muscle–fluid–structure simulations. *Integr. Comp. Biol.* **55**, 901-911.

Bringley, T. T. and Peskin, C. S. (2008). Validation of a simple method for representing spheres and slender bodies in an immersed boundary method for Stokes flow on an unbounded domain. *J. Comput. Phys.*, **227**, 5397-5425.

Cheer, A. Y. L. and Koehl, M. A. R. (1987). Paddles and rakes: fluid flow through bristled appendages of small organisms. *J. Theor. Biol.* **129**, 17-39.

Cheer, A., Cheung, S., Hung, T.-C., Piedrahita, R. H. and Sanderson, S. L. (2012). Computational fluid dynamics of fish gill rakers during crossflow filtration. *Bull Math Biol.* **74**, 981-1000.

Childs, H. (2013). VisIt: An end-user tool for visualizing and analyzing very large data. In *High Performance Visualization: Enabling Extreme-Scale Scientific Insight* (E. W. Bethel, H. Childs and C. Hansen), pp. 357-372. Boca Raton: Taylor and Francis Publishing.

Davidi, G. and Weihs, D. (2012). Flow around a comb wing in low-Reynolds-number flow. *AIAA J.* **50**, 249-252.

Ellington, C. P. (1975). *Swimming and Flying in Nature*, Vol. 2. New York: Plenum Press.

Ellington, C. P. (1980). Wing mechanics and take-off preparation of thrips (Thysanoptera). *J. Exp. Biol.* **85**, 129-136.

Geuzaine, C. and Remacle, J.-F. (2009). Gmsh: A 3-D finite element mesh generator with built-in pre-and post-processing facilities. *Int. J. Numer. Methods Eng.* **79**, 1309-1331.

Gorham, P. W. (2013). Ballooning spiders: the case for electrostatic flight. *arXiv* Preprint. arXiv:1309.4731.

Griffith, B. E. and Luo, X. (2012). Hybrid finite difference/finite element version of the immersed boundary method. *Int. J. Numer. Meth. Engng.* doi: 10.1002/nme.

Griffith, B. E., Hornung, R. D., McQueen, D. M. and Peskin, C. S. (2007). An adaptive, formally second order accurate version of the immersed boundary method. *J. Comput. Phys.* **223**, 10-49.

Huber, J. and Baquero, E. (2007). Review of Eustochus, a rarely collected genus of Mymaridae (Hymenoptera). *J. Entomol. Soc. Ontario* **138**, 3.

Huber, J. T. and Noyes, J. S. (2013). A new genus and species of fairyfly, Tinkerbella nana (Hymenoptera, Mymaridae), with comments on its sister genus Kikiki, and discussion on small size limits in arthropods. *J. Hymenopt. Res.* **32**, 17-44.

Huber, J. T., Mendel, Z., Protasov, A. and La Salle, J. (2006). Two new Australian species of Stethynium (Hymenoptera: Mymaridae), larval parasitoids of Ophelimus maskelli (Ashmead) (Hymenoptera: Eulophidae) on Eucalyptus. *J. Nat. Hist.* **40**, 1909-1921.

Huber, J. T., Gibson, G. A., Bauer, L. S., Liu, H. and Gates, M. (2008). The genus Mymaromella (Hymenoptera: Mymarommatidae) in North America, with a key to described extant species. *J. Hymenopt. Res.* **17**, 175-194.

Jones, S. K. (2016). A computational fluid dynamics study of the smallest flying insects. PhD thesis, The University of North Carolina at Chapel Hill.

Koehl, M. A. R. (1993). Hairy little legs: feeding, smelling and swimming at low Reynolds numbers. *Contemp. Math.* **141**, 33-64.

Kolomenskiy, D., Moffatt, H. K., Farge, M. and Schneider, K. (2010). Vorticity generation during the clap–fling–sweep of some hovering insects. *Theor. Comput. Fluid Dyn.* **24**, 209-215.

Kolomenskiy, D., Moffatt, H. K., Farge, M. and Schneider, K. (2011). Two-and three-dimensional numerical simulations of the clap–fling–sweep of hovering insects. *J. Fluid Struct.* **27**, 784-791.

Kuethe, A. M. (1975). *Swimming and Flying in Nature*, Vol. 2. New York: Plenum Press.

Lehmann, F.-O. and Pick, S. (2007). The aerodynamic benefit of wing–wing interaction depends on stroke trajectory in flapping insect wings. *J. Exp. Biol.* **210**, 1362-1377.

Lehmann, F.-O., Sane, S. P. and Dickinson, M. (2005). The aerodynamic effects of wing-wing interaction in flapping insect wings. *J. Exp. Biol.* **208**, 3075-3092.

Lighthill, M. J. (1973). On the Weis-Fogh mechanism of lift generation. *J. Fluid Mech.* **60**, 1-17.

Lin, N., Huber, J. T. and LaSalle, J. (2007). *The Australian genera of Mymaridae (Hymenoptera: Chalcidoidea)*. Auckland, New Zealand: Magnolia Press.

Loudon, C., Best, B. A. and Koehl, M. A. R. (1994). When does motion relative to neighboring surfaces alter the flow through an array of hairs? *J. Exp. Biol.* **193**, 233-254.

Maxworthy, T. (1979). Experiments on the Weis-Fogh mechanism of lift generation by insects in hovering flight. Part 1. Dynamics of the 'fling'. *J. Fluid Mech.* **93**, 47-63.

Melika, G. and Thuroczy, C. (2002). Parasitic wasps: evolution, systematics, biodiversity and biological control: International Symposium:" Parasitic hymenoptera: taxonomy and biological control", 14-17 mMay y2001. Kőszeg, Hungary: Agroinform.

Miller, L. A. and Peskin, C. S. (2005). A computational fluid dynamics study of 'clap and fling' in the smallest insects. *J. Exp. Biol.* **208**, 195-212.

Miller, L. A. and Peskin, C. S. (2009). Flexible clap and fling in tiny insect flight. *J. Exp. Biol.* **212**, 3076-3090.

Peskin, C. S. (2002). The immersed boundary method. *Acta Numerica* **11**, 479-517.

Santhanakrishnan, A., Robinson, A. K., Jones, S., Low, A. A., Gadi, S., Hedrick, T. L. and Miller, L. A. (2014). Clap and fling mechanism with interacting porous wings in tiny insect flight. *J. Exp. Biol.* **217**, 3898-3909.

Schneider, C. A., Rasband, W. S. and Eliceiri, K. W. (2012). NIH Image to ImageJ: 25 years of image analysis. *Nat. Methods* **9**, 671-675.

Spedding, G. R. and Maxworthy, T. (1986). The generation of circulation and lift in a rigid two-dimensional fling. *J. Fluid Mech.* **165**, 247-272.

Sunada, S., Takashima, H., Hattori, T., Yasuda, K. and Kawachi, K. (2002). Fluid-dynamic characteristics of a bristled wing. *J. Exp. Biol.* **205**, 2737-2744.

Valmalette, J. C., Raad, H., Qiu, N., Ohara, S., Capovilla, M. and Robichon, A. (2015). Nano-architecture of gustatory chemosensory bristles and trachea in Drosophila wings. *Sci. Rep.* **5**, 14198.

Weihs, D. and Barta, E. (2008). Comb-wings for flapping flight at extremely low Reynolds numbers. *AIAA J.* **46**, 285-288.

Weis-Fogh, T. (1973). Quick estimates of flight fitness in hovering animals, including novel mechanisms for lift production. *J. Exp. Biol.* **59**, 169-230.